

Effects of Enoyl-Acyl Protein Carrier Reductase Mutations on Physiochemical Interactions with Isoniazid: Molecular Dynamics Simulation

Yee Siew Choong^{1,*}, Habibah A. Wahab²

¹ Institute for Research in Molecular Medicine, Universiti Sains Malaysia, 11800 Penang, Malaysia.

² Pharmaceutical Design and Simulation Laboratory, School of Pharmaceutical Sciences, Universiti Sains Malaysia, 11800 Minden, Penang, Malaysia

*E-mail: yeesiew@usm.my

Received: 5 May 2011 / Accepted: 25 July 2011 / Published: 1 September 2011

The resistance strains of *Mycobacterium tuberculosis* have complicated the tuberculosis management and therapy. Prior to the discovery of a more effective therapy, it is crucial to understand the molecular basis and physiochemical interaction for drug resistance with its target. In this study, molecular dynamics simulation was employed to elucidate the molecular events which lead to isoniazid (first line drug of tuberculosis) resistance in *M. tuberculosis* mutant enoyl-acyl carrier protein reductase (InhA). This paper reported the results from molecular dynamics simulation of wild type and seven mutant types (I16T, I21T, I21V, I47T, V78A, S94A and I95P) InhA in complex with its inhibitor, isonicotinic acyl-NADH (INADH, which is the activated form of the prodrug isoniazid). It was found that due to the hydrophobicity changed of the mutated residues in mutant InhA, both INADH and mutant InhA have to rearrange their conformations in order to accommodate and stabilize the steric and electrostatic effects. Besides that, it is interesting to find that all mutated residues have the reduction in side chain volume. This has contributed to a larger room for the structural fluctuation and rearrangement among INADH and mutant InhA, and thus the decreased in binding affinity of INADH in mutant InhA. The atomic fluctuation and structural instabilities in all mutants InhA-INADH compared with that of wild type InhA-INADH are correlated with experimental finding where InhA mutations caused low level of isoniazid resistance.

Keywords: *Mycobacterium tuberculosis*, INADH, isoniazid resistance, mutant enoyl-acyl carrier protein reductase, molecular dynamics simulation

1. INTRODUCTION

Tuberculosis (TB) is an infectious disease caused by *Mycobacterium tuberculosis* and has accounted up to 26% of avoidable human deaths [1]. Statistic showed the trend of a staggering one

billion newly infected and 36 million patients in the coming two decades [2]. Isoniazid (isonicotinic acid hydrazide; INH) is an essential compound of global TB management program [3]. However, the continuing rise in the incidence of multi drug resistant TB (resistant to ≥ 1 anti-TB drug including INH) [4], extensively drug resistant TB (resistant to INH and rifampicin, and in addition to ≥ 3 classes of second line anti-TB drugs), extremely drug-resistant TB (resistant to all first and second line anti-TB drugs) and totally drug resistant TB show the urgent need of a basic science to address the key contribution in new diagnostics, new drugs and ultimately development vaccine to protect the future generation from TB [5-8].

Early studies have demonstrated direct correlation of INH on the inhibition of mycolic acids (specifically saturated fatty acids of > 26 carbons and mono-unsaturated long-chain fatty acids) biosynthesis of mycobacterial cell wall. These indicating that the enzyme involved in the biosynthesis of mycolic acids is the target protein of INH [9-12]. Subsequent studies have also identified the target and action site of INH is *inhA* gene product, namely enoyl-acyl carrier protein reductase (InhA), is catalyzing the synthesis of the fatty acids [13-19].

Different mechanisms of INH activation have been reviewed by Scior *et al.* [20]. More studies have also demonstrated that the mutations within *katG* in *M. tuberculosis* are common in INH resistant strains [21]. These suggest that INH is a prodrug which requires KatG (*katG* product; a catalase-peroxidase enzyme) in order to be activated and reacts with the co-factor, NADH, to form isonicotinic acyl-NADH (INADH), which in turn the genuine inhibitor of InhA [22-26]. Besides *katG*, mutations in several genes of *M. tuberculosis* are also involved in INH resistance, e.g. *inhA*, *ahpC*, *kasA* and *ndh* [18,27]. The mutations within *inhA* have been reported up to 32% in INH resistant strains [13,28-30]. Mutations in *katG* and *inhA* account for up to 80% of INH resistant strains [28,31] whereas the mutations in *katG* alone account for the majority of INH resistant strains [24,27]. Studies also showed that low level INH resistant strains had single point mutation in mutant type (MT) InhA (I16T, I21T, I21V, I47T, V78A, S94A and I95P) [32-35]. X-ray crystallographic results [36-38] also showed that S94A, I21V and I47T InhA have decreased in NADH binding affinity.

Therefore, prior to the discovery and design of new therapeutics, the understanding of the physiochemical interactions between a drug and its target is important as showed by many studies [39-45]. In this research, molecular dynamics simulation was performed on INADH-InhA complex. Both wild type (WT) and seven point mutations of InhA were considered. All mutated InhA residues have the decreased in the side chain volume and hydrophobicity changed as compared with the wild type. These contributed to the gross conformational change and the lost of water mediated hydrogen bonding of protein and inhibitor. These physiochemical interactions changed between INADH and mutant InhA have therefore, attributed to the low level of isoniazid resistance in mutant type (MT) InhA.

2. METHODOLOGY

MD simulation was performed using Amber8 [46] with Amber 2003 force field [47], parm99.dat parameter set [48], TIP3P water potential parameters [49] and NPT ensembles. Periodic

boundary condition was employed with primary cut off at 12.0 Å. Electrostatic interaction was addressed using PME method.

Table 1. The number of water molecules and total atoms in MD simulation of INADH in complex with WT and MT (I16T, I21T, I21V, I47T, V78A, S94A and I95P) InhA.

System	Number of water molecules	Total numbers of atoms
INADH-WT	7754	27559
INADH-I16T	7747	27533
INADH-I21T	7756	27560
INADH-I21V	7755	27559
INADH-I47T	7751	27545
INADH-V78A	7754	27553
INADH-S94A	7906	27957
INADH-I95P	7753	27551

Each complex was named with INADH and InhA in the prefix (e.g. wild type InhA in complex with INADH was named INADH-WT). WT initial coordinates was obtained from PDB (PDB id 1ZID) while the initial structure of INADH in complex with WT was obtained from docking simulation (as described in earlier work [50]) and refined with InsightII's Builder Module (Accelrys Inc., San Diego). The initial coordinates of S94A was obtained from PDB (PDB id 1ENZ) while the structure of INADH in complex with S94A was setup alike INADH in complex with WT. I16T, I21T, I21V, I47T, V78A and I95P mutant type (MT) InhA were mutated from INADH-WT complex using InsightII's Homology Module (Accelrys Inc., San Diego) to generate INADH-I16T, INADH-I21T, INADH-I21V, INADH-I47T, INADH-V78A and INADH-I95P complex. INADH partial charges were assigned using MOPAC 6.00 (Steward, J. J., Fujitsu Limited, Tokyo). All atoms in INADH-InhA were treated explicitly and contained (i) one Na⁺ ion as neutralizing counterion, (ii) all water molecules from crystal structures and, (iii) 10 Å truncated octahedron water box. Table 1 shows the number of water molecules and total number of atoms in each system. Each system was subsequently energy minimized under steepest descent method followed by conjugate gradient for 1,000 steps for each run. The MD parameters were: 5,000,000 of 2 fs time step; warmed up from 0 K to and maintained at 300 K by Berendsen thermostat [51] with the coupling constant of 0.5 ps and SHAKE algorithm [52] was turned on throughout the simulation. A total of 200 ps were allowed for the system to equilibrate and 201-10,000 ps were the production run.

3. RESULTS AND DISCUSSION

Earlier studies have showed that I16T, I47T and S94A InhA have lower binding affinity with NADH compared with that of WT InhA [36-38]. Similar finding was also observed from previous calculation where INADH has a lower binding affinity with S94A InhA than that of WT InhA [26].

Therefore, we hypothesized that INADH will also have lower binding affinity with I16T, I21T, I21V, I47T, V78A and I95P MT InhA. In this study, we performed MD simulations to elucidate the molecular events which lead to INH resistance as well as to identify the molecular aspects of INADH in mutant InhA affinity differences.

Table 2. The root mean square fluctuation (RMSF) and deviation (RMSD) during MD simulation.

System	RMSF (Å)		RMSD with WT crystal structure (Å)	
	C_{α} atom	INADH	C_{α} atom	INADH
INADH-WT	1.8 ± 0.1	0.8 ± 0.2	1.8 ± 0.2	1.5 ± 0.1
INADH-I16T	1.8 ± 0.1	1.1 ± 0.2	1.7 ± 0.2	1.7 ± 0.2
INADH-I21T	2.5 ± 0.1	0.8 ± 0.2	1.8 ± 0.2	1.6 ± 0.2
INADH-I21V	1.3 ± 0.1	0.7 ± 0.2	1.9 ± 0.2	1.7 ± 0.2
INADH-I47T	5.1 ± 0.2	1.9 ± 0.2	2.3 ± 0.5	1.9 ± 0.2
INADH-V78A	3.5 ± 0.2	1.6 ± 0.2	2.3 ± 0.5	1.5 ± 0.1
INADH-S94A	1.6 ± 0.2	1.6 ± 0.2	2.2 ± 0.4	2.8 ± 0.8
INADH-I95P	1.5 ± 0.1	0.8 ± 0.2	1.8 ± 0.2	1.7 ± 0.2

Table 3. The WT and MT side chain volume (calculated using HyperChem 7.0, Hypercube Inc., FL) and distance from INADH.

InhA	Residue	Distance from INADH (Å)	Side chain volume (Å ³)
WT	I16	9.9 ± 0.3	307.8
MT	I16T	9.0 ± 1.3	232.7
WT	I21	7.1 ± 0.3	307.8
MT	I21T	6.8 ± 0.3	232.7
WT	I21	7.1 ± 0.3	307.8
MT	I21V	7.1 ± 0.3	262.1
WT	I47	15.6 ± 0.4	307.8
MT	I47T	14.1 ± 0.5	232.7
WT	V78	20.9 ± 0.6	262.1
MT	V78A	21.2 ± 0.5	150.5
WT	S94	6.0 ± 0.3	177.0
MT	S94A	7.6 ± 0.9	150.5
WT	I95	5.7 ± 0.3	307.8
MT	I95P	6.5 ± 0.4	278.8

Table 2 shows carbon backbone (C_{α}) of MT had higher fluctuation compared with that of WT. This could be explained as amino acid mutation in MT will lead to slight backbone structural rearrangement to minimise and avoid the steric clashes on the side chains. Point mutation in all MT (I16T, I21T, I21V, I47T, V78A, S94A and I95P) also led to the formation of a larger space (Table 3). This has allowed the side chain of the mutated amino acid to fluctuate. Thus, decreased the interaction of INADH with the mutated amino acid and contributed to a higher fluctuation on both INADH and MT InhA. These have therefore, decreased the INADH binding affinity with MT InhA. I16T, I21T, I47T, S94A and I95P point mutations has changed the hydrophobicity profile from WT, which also caused the greater fluctuations of C_{α} atom in order to compensate the subtle balance between repulsion and dispersion effects. The fluctuation of INADH in MT is also greater than that of WT (Table 2) due to the hydrophobicity changes in the binding pocket.

Table 4. Clustering of INADH-InhA complex and INADH.

System	No. of cluster	Population in top cluster	RMSD from centroid (Å)
INADH-WT	3	7533	1.1
INADH-I16T	4	4597	1.1
INADH-I21T	19	4021	1.1
INADH-I21V	4	4750	1.1
INADH-I47T	5	3902	1.1
INADH-V78A	13	2017	1.2
INADH-S94A	9	2475	1.1
INADH-I95P	11	3693	1.1
INADH in WT	4	4187	0.4
INADH in I16T	9	2490	0.4
INADH in I21T	4	6392	0.4
INADH in I21V	5	4407	0.4
INADH in I47T	10	1746	0.4
INADH in V78A	6	3500	0.4
INADH in S94A	16	2207	0.4
INADH in I95P	7	2768	0.5

Investigation from MD trajectories on the distance of INADH from the mutated residue showed variation due to the mutation (Table 3). It is interesting to find that all point mutations contributed to a decrease of side chain volume (Table 3) and thus created a larger space between the mutated residue and INADH. It is thus the distance of INADH deviated more compared to WT. The hydrophilic to hydrophobic mutation (S94 to S94A) has forced the highly polar pyrophosphate region of INADH to relocate away. In contrast, the mutation of hydrophobic to hydrophilic residue (I21 to I21T and I47 to I47T) has forced the highly polar pyrophosphate region of INADH to move nearer to the mutated residue. Hydrophobic to hydrophilic mutation of isoleucine to threonine at residue 16 showed the same

observation where the highly polar ribose hydroxyl region of INADH moved nearer to I16T. The distance of INADH was found to be further in V78A as compared with that in WT.

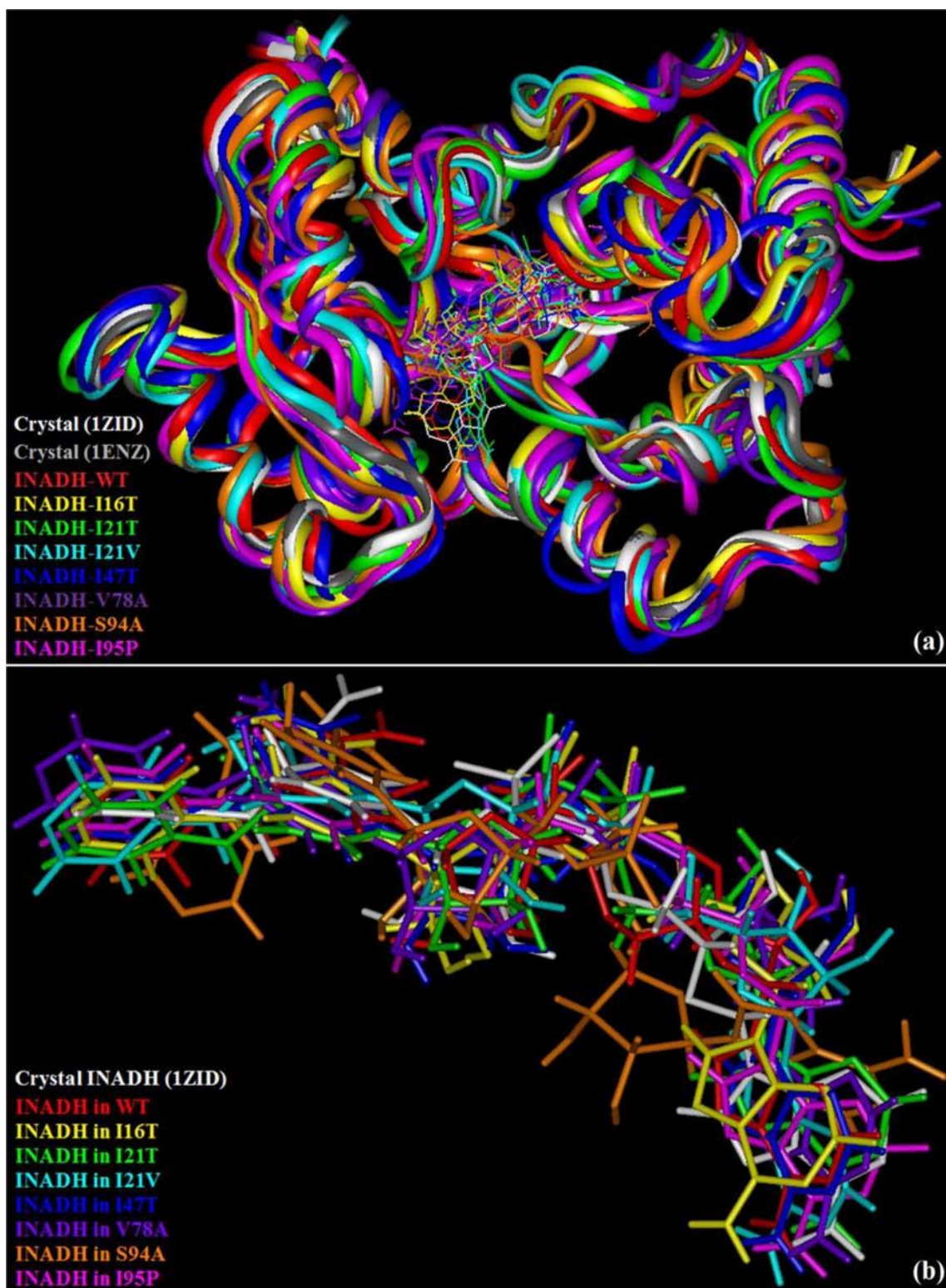


Figure 1. The member with the closet RMSD value from the centroid of the most populated cluster for a) INADH-InhA complex, and b) INADH in InhA. The InsightII modeling package was used.

This might be attributed to the change from the bulkier to smaller side chain in V78A (Table 3) which created extra void and distance from INADH. I95P mutation should bring INADH closer to it but results showed otherwise. This might be due to a water exchange and mediation into the void from I95 to I95P mutation for INADH-I95P interaction.

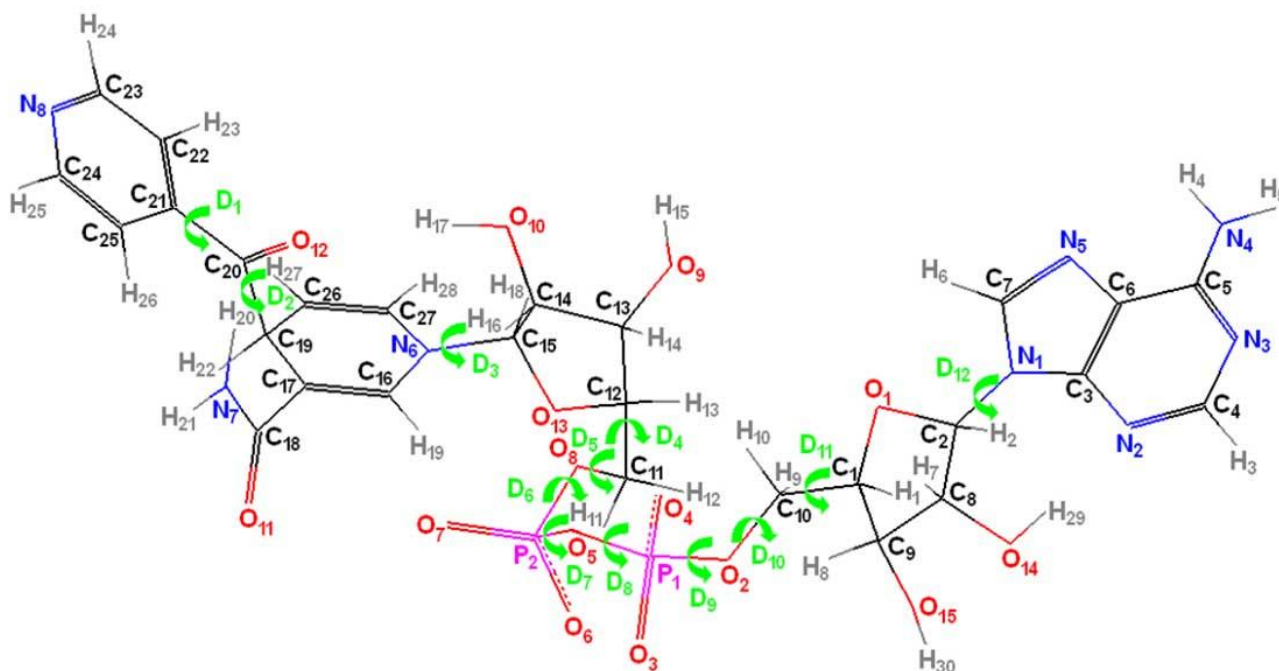


Figure 2. The dihedral angle for INADH main chain. The InsightII modeling package was used.

In order to identify and classify cluster of similar conformations and variables from during MD simulations, cluster analysis was performed using MMTSB Tool Set [53]. Analysis showed that the number of cluster in INADH-WT complex or INADH in WT were lower compared with that of in mutated system (Table 4; Fig. 1). Dihedral angle analysis in INADH main chain (Fig. 2) was performed to describe the contribution of INADH conformation which leads to the binding affinity differences in WT and MT InhA. It was found that INADH main chain rotations in MT were different with that of in WT, where the INAFH in MT took place at the dihedral angle pyrophosphate region (Figures in Supplementary Material). This affected the conformation in both pyridine and adenine end of INADH and thus the overall INADH conformation. The vigorous dihedral angle rotations might again be attributed to the hydrophobicity and space changes due to InhA point mutation (Fig. 3).

The active site of the protein contains typically around 20 water molecules (21.0 ± 2.6 , 23.0 ± 3.2 , 26.7 ± 2.9 , 28.2 ± 2.6 , 24.7 ± 3.8 , 25.9 ± 2.5 , 19.2 ± 5.4 , 24.7 ± 3.0 water molecules within 3.2 \AA from INADH in WT, I16T, I21T, I21V, I47T, V78A, S94A and I95P, respectively). The radial distribution functions were therefore calculated with respect to water oxygen atom to investigate the contribution of water molecules between INADH and InhA. For INADH radial distribution function plots with peaks occurred after the hydrogen bond cutoff of 3.2 \AA [54] was consider free from solvation as in not making any contact (in term of hydrogen bonding) with any water molecule.

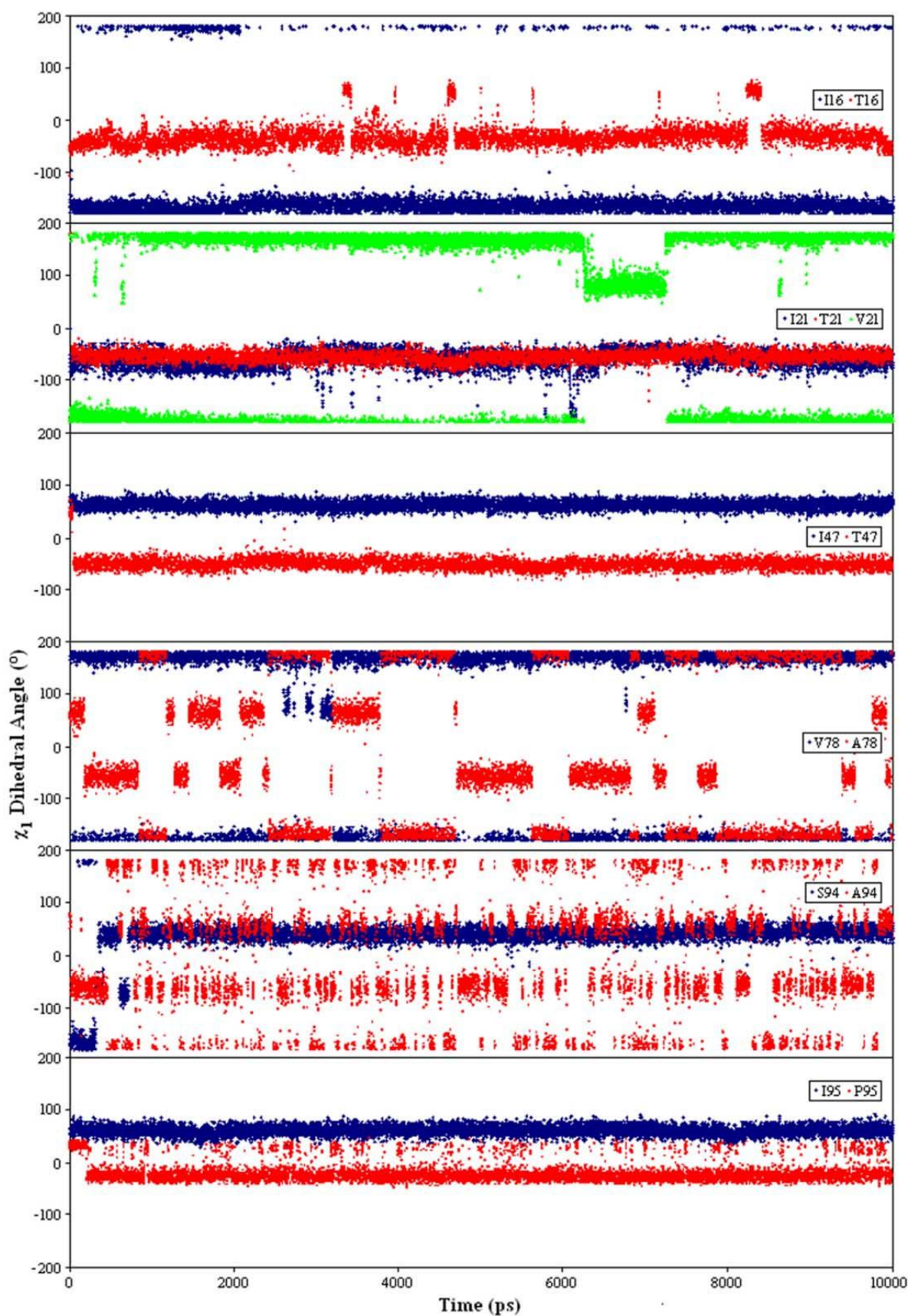


Figure 3. Graphical plot of χ_1 torsional fluctuation of WT and MT residues (I16 and T16; I21 and T21/V21; I47 and T47; V78 and A78; S94 and A94; I95 and P95) as a function of time.

Table 5. The radial distribution functions (RDF) analysis with respect to water oxygen atom. Only the pair distribution between INADH and water oxygen atom with the pronounced sharp peak within 3.2 Å showed here.

INADH atom	InhA	Distance (Å)	Intensity
O3	WT	2.625	2.659
O3	I16T	2.625	1.365
O3	I21T	2.675	1.380
O3	I21V	2.625	1.296
O3	I47T	2.675	2.513
O3	V78A	2.625	1.604
O3	S94A	2.625	1.112
O3	I95P	2.675	1.595
O4	WT	2.675	1.910
O4	I16T	2.625	2.964
O4	I21T	2.625	2.896
O4	I21V	2.675	2.901
O4	I47T	2.675	2.804
O4	V78A	2.625	2.502
O4	I95P	2.675	2.205
O6	WT	2.675	1.683
O6	I16T	2.625	2.684
O6	I21T	2.675	2.754
O6	I21V	2.625	2.941
O6	I47T	2.675	2.718
O6	V78A	2.625	2.613
O6	I95P	2.675	2.059
O7	WT	2.625	2.520
O7	I16T	2.675	1.141
O7	I21T	2.675	1.306
O7	I21V	2.625	1.505
O7	I47T	2.625	2.961
O7	V78A	2.625	1.927
O7	S94A	2.625	2.120
O7	I95P	2.625	2.045

This radial distribution function analysis gives, in general, an idea of the possible or potential specific water bridging/mediating interaction between INADH and InhA. The water mediated interaction analysis is importance as studies have shown that water plays an important role in

mediating many systems [55-57]. Results (Table 5) showed the potential of water mediated effects in all systems.

Table 6. The hydrogen bond analysis in INADH-InhA complex with hydrogen bond that occupied at least 80% during the MD simulation

System	%	Atom involved	Distance (Å)
INADH-WT	99.0	O ₆ (INADH) - H _{G1} (Thr196)	2.7 ± 0.1
	93.2	H(Ala22) - O(Wat275)	3.0 ± 0.1
	90.1	H(Asp150) - O(Wat276)	3.0 ± 0.1
	88.4	H _{H21} (Ala22) - O(Wat7445)	2.9 ± 0.1
	87.1	O ₇ (INADH) - H ₂ (Wat275)	3.0 ± 0.1
	80.2	O ₁₁ (INADH) - H(Ile194)	2.8 ± 0.2
INADH-I16T	94.6	H(Ala22) - O(Wat275)	3.0 ± 0.1
	87.3	H(Phe41) - O(Wat285)	2.6 ± 0.1
	82.5	H(Asp42) - O(Wat285)	3.0 ± 0.1
	81.7	H(Arg43) - O(Wat285)	3.0 ± 0.1
INADH-I21V	98.7	O ₃ (INADH) - H _G (Ser20)	2.6 ± 0.1
	95.5	H _{D1} (His93) - O(Wat295)	2.9 ± 0.1
	85.3	O ₁₀ (INADH) - O(Met147)	2.8 ± 0.2
	83.0	O ₇ (INADH) - H(Val21)	2.9 ± 0.1
INADH-V78A	81.1	O ₃ (INADH) - H _G (Ser20)	2.7 ± 0.1
INADH-S94A	99.6	O ₄ (INADH) - H _{G1} (Thr196) O ₃ (INADH) -	2.6 ± 0.1
	97.1	H _G (Ser20) O ₆ (INADH) - H(Ala22)	2.6 ± 0.1
	96.2	H _{D1} (His93) - O(Wat294)	2.9 ± 0.1
	89.3		2.7 ± 0.1
INADH-I95P	84.5	O ₃ (INADH) - H _G (Ser20)	2.7 ± 0.1

Therefore, further comprehensive investigation for direct and water mediated hydrogen bond between INADH and InhA were examined.

This analysis was performed in order to study the contribution of water molecules towards INADH binding affinity and to identify specific water molecule which might mediate the hydrogen bonding. Only those hydrogen bonds which occurred at 80% or more during the production run were considered as permanent or persistent hydrogen bond.

Result (Table 6) showed that there were total 2, 3, 1, 3, 1 direct hydrogen bond between INADH and WT, I21V, V78A, S94A and I95P, respectively. No direct persistent hydrogen bond between INADH and I16T, I21T and I47T, respectively were found throughout MD simulations. No similar residue in either WT or MT was found to be hydrogen bond with INADH suggesting that INADH in MTs were orientated differently as in WT. The hydrogen bond analysis also demonstrated the occurrence of water molecule mediated/bridged INADH-InhA hydrogen bond in only INADH-WT system by Wat275. This water mediated hydrogen bond analysis found different observation that that of earlier study by Pantano [58] on NADH-S94A, but this different need future study as it is two difference systems.

In general, the results from present study are in line with another related study on NADH-WT/I16T/I21V and the proposed mechanism of INH resistant [26,36-38,59,60]. The investigation on INADH-WT and INADH-MTs systemx have one common finding where the low level of INH resistant was linked to the decrease NADH affinity attributed by InhA point mutations.

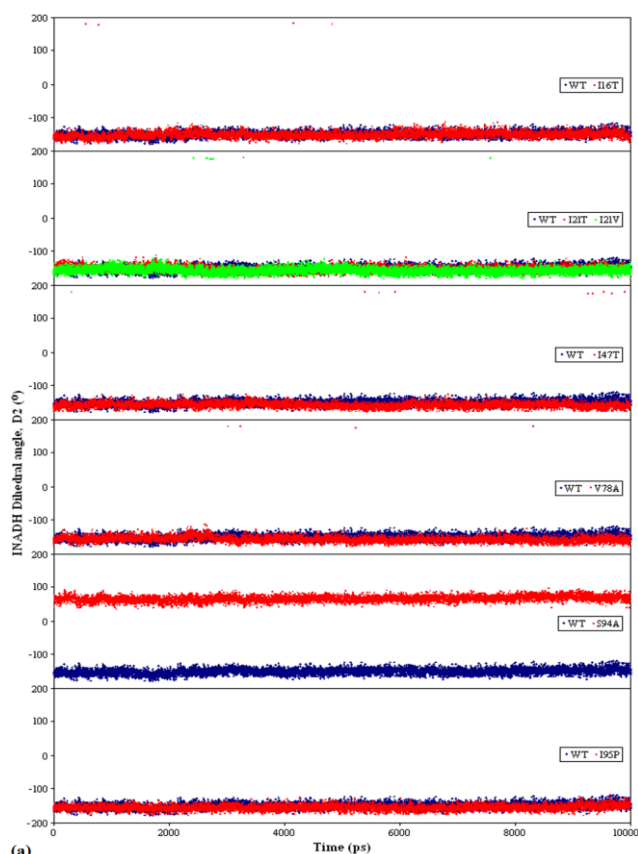
4. CONCLUSIONS

This study utilized MD simulation to elucidate the molecular events in the physiochemical interactions changed that lead to low level isoniazid resistance. Results showed that the main mechanism that contributed to the resistant including the fluctuation of InhA, the flexibility of InhA-INADH and, the water mediating effect, which caused the decrease of INADH binding affinity in mutated proteins.

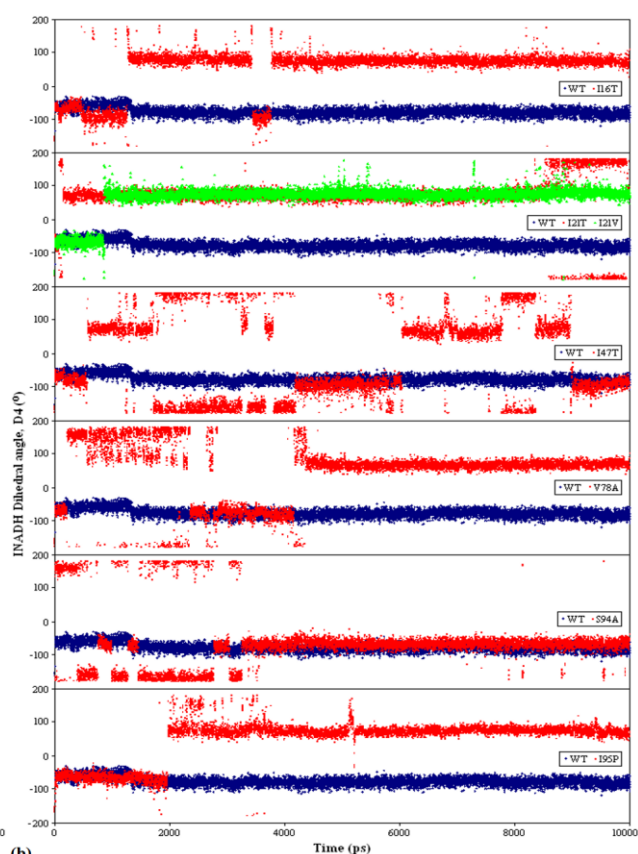
The decreased of INADH binding affinity in mutant InhA are due to the consequence of the point mutation which has changed the hydrophobicity of the mutated residue as well as created more space, and thus the structural rearrangement of InhA and INADH. Evolutionally, ligand was optimized to have favourable interaction free energy of binding with wild type InhA. However, mutant type has more pronounced flexibility giving rise to decreased affinity toward inhibitors. Thus, design of novel inhibitors remains a challenge for future involves proteins engineering in term of structure and flexibility. The information and data gathered from this study would be able to improve the present understanding about the ligand binding characteristics and assist in future *in silico* studies of other potential lead ligand.

SUPPORTING INFORMATION AVAILABLE

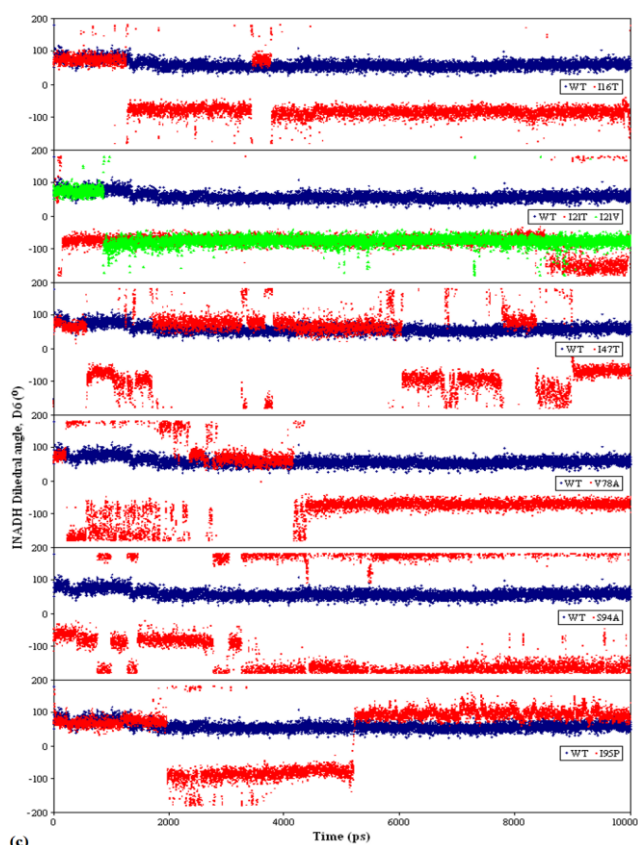
The dihedral angle a) D2, b) D4, c) D6, d) D7, e) D8, f) D9, g) D10, and h) D11 rotation of INADH in WT compared with that of in MT InhA with the function of time.



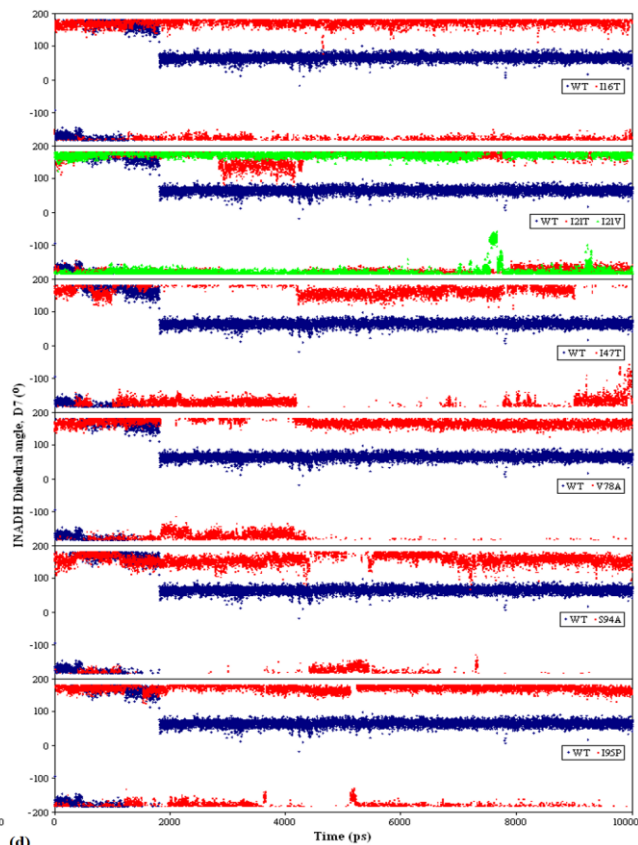
A



B



C



D

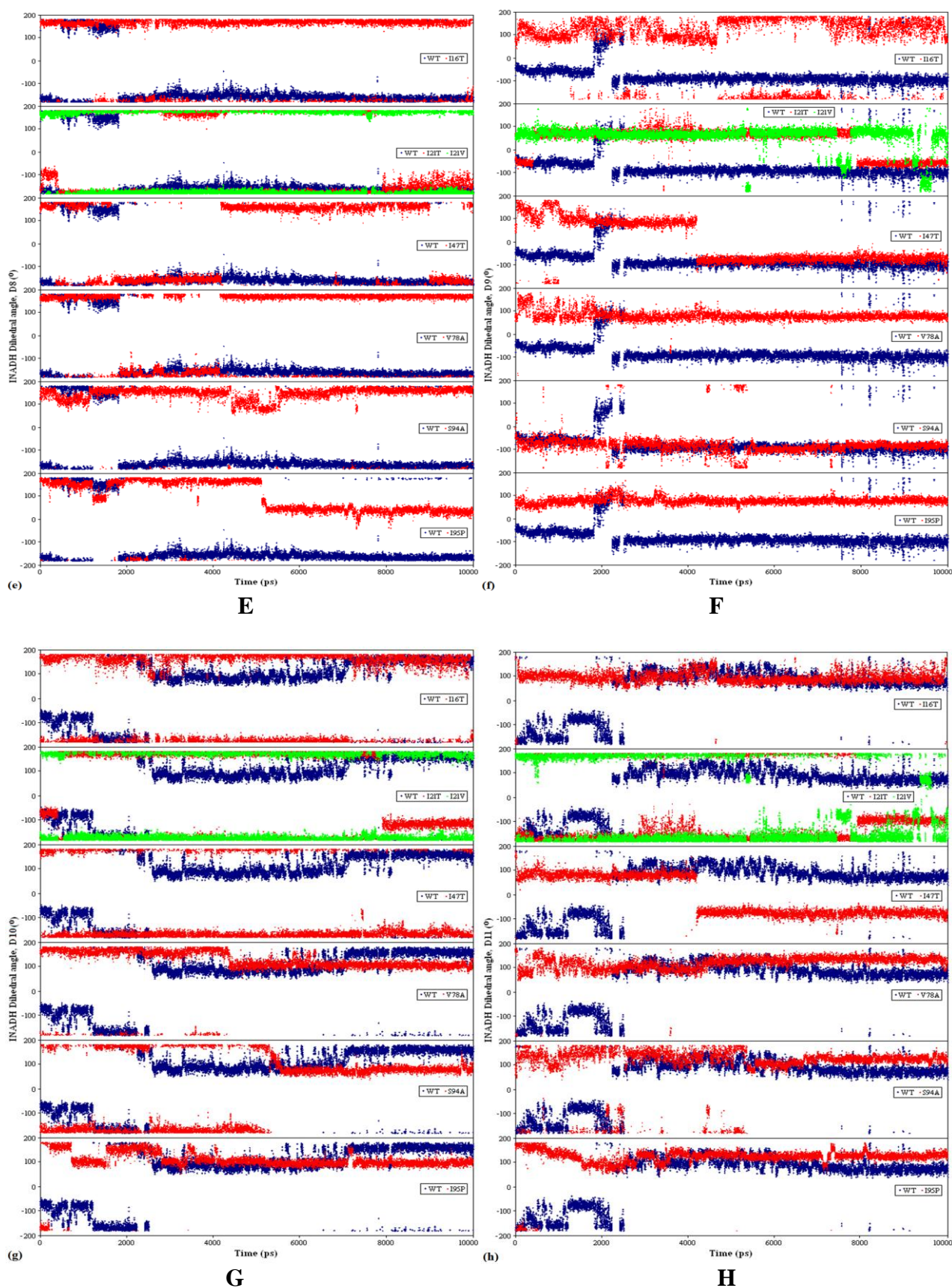


Figure S1. The dihedral angle a) D2, b) D4, c) D6, d) D7, e) D8, f) D9, g) D10, and h) D11 rotation of INADH in WT compared with that of in MT InhA with the function of time.

ACKNOWLEDGEMENTS

This work was supported by University Sains Malaysia Short Term Grant (304/CIPPM/639016). We thank MIMOS for providing the computing time for this work.

References

1. J. E. Gomez and J. D. McKinney, *Tuberculosis (Edinb)*, 84 (2004) 29
2. N. Scherr, S. Honnappa, G. Kunz, P. Mueller, R. Jayachandran, F. Winkler, J. Pieters and M. O. Steinmetz, *Proc. Natl. Acad. Sci. USA*, 104 (2007) 12151
3. C. J. Wei, B. Lei, J. M. Musser and S. C. Tu, *Antimicrob. Agents Chemother.*, 47 (2003) 670
4. W. C. Yam, C. M. Tam, C. C. Leung, H. L. Tong, K. H. Chan, E. T. Leung, K. C. Wong, W. W. Yew, W. H. Seto, K. Y. Yuen and P. L. Ho, *J Clin Microbiol*, 42 (2004) 4438
5. N. R. Gandhi, A. Moll, A. W. Sturm, R. Pawinski, T. Govender, U. Laloo, K. Zeller, J. Andrews and G. Friedland, *Lancet*, 368 (2006) 1575
6. G. B. Migliori, R. Loddenkemper, F. Blasi and M. C. Raviglione, *Eur Respir J*, 29 (2007) 423
7. N. S. Shah, A. Wright, G. H. Bai, L. Barrera, F. Boulahbal, N. Martin-Casabona, F. Drobniewski, C. Gilpin, M. Havelkova, R. Lepe, R. Lumb, B. Metchock, F. Portaels, M. F. Rodrigues, S. Rusch-Gerdes, A. Van Deun, V. Vincent, K. Laserson, C. Wells and J. P. Cegielski, *Emerg Infect Dis*, 13 (2007) 380
8. M. R. Masjedi, P. Farnia, S. Sorooch, M. V. Pooramiri, S. D. Mansoori, A. Z. Zarifi, A. Akbarvelayati and S. Hoffner, *Clin Infect Dis*, 43 (2006) 841
9. F. G. Winder and P. B. Collins, *J. Gen. Microbiol.*, 63 (1970) 41
10. K. Takayama, L. Wang and H. L. David, *Antimicrob. Agents Chemother.*, 2 (1972) 29
11. K. Takayama, H. K. Schnoes, E. L. Armstrong and R. W. Boyle, *J Lipid Res*, 16 (1975) 308
12. L. A. Davidson and K. Takayama, *Antimicrob Agents Chemother*, 16 (1979) 104
13. A. Telenti, N. Honore, C. Bernasconi, J. March, A. Ortega, B. Heym, H. E. Takiff and S. T. Cole, *J. Clin. Microbiol.*, 35 (1997) 719
14. A. Banerjee, E. Dubnau, A. Quemard, V. Balasubramanian, K. S. Um, T. Wilson, D. Collins, G. de Lisle and W. R. Jacobs, Jr., *Science*, 263 (1994) 227
15. A. Quemard, C. Lacave and G. Laneelle, *Antimicrob. Agents Chemother.*, 35 (1991) 1035
16. J. Y. Wang, R. M. Burger and K. Drlica, *Antimicrob Agents Chemother*, 42 (1998) 709
17. Z. Fang, C. Doig, A. Rayner, D. T. Kenna, B. Watt and K. J. Forbes, *J Clin Microbiol*, 37 (1999) 998
18. C. Vilcheze, H. R. Morbidoni, T. R. Weisbrod, H. Iwamoto, M. Kuo, J. C. Sacchettini and W. R. Jacobs, Jr., *J. Bacteriol.*, 182 (2000) 4059
19. S. S. Poletto, I. O. da Fonseca, L. P. de Carvalho, L. A. Basso and D. S. Santos, *Protein Expr. Purif.*, 34 (2004) 118
20. T. Scior, I. Meneses Morales, S. J. Garces Eisele, D. Domeyer and S. Laufer, *Arch. Pharm. (Weinheim)*, 335 (2002) 511
21. B. Heym, P. M. Alzari, N. Honore and S. T. Cole, *Mol. Microbiol.*, 15 (1995) 235
22. A. Quemard, J. C. Sacchettini, A. Dessen, C. Vilcheze, R. Bittman, W. R. Jacobs, Jr. and J. S. Blanchard, *Biochemistry*, 34 (1995) 8235
23. Y. Zhang, S. Dhandayuthapani and V. Deretic, *Proc. Natl. Acad. Sci. USA*, 93 (1996) 13212
24. M. H. Cynamon, Y. Zhang, T. Harpster, S. Cheng and M. S. DeStefano, *Antimicrob. Agents Chemother.*, 43 (1999) 2922
25. B. Lei, C. J. Wei and S. C. Tu, *J. Biol. Chem.*, 275 (2000) 2520
26. H. A. Wahab, Y. S. Choong, P. Ibrahim, A. Sadikun and T. Scior, *J Chem Inf Model*, 49 (2009) 97
27. M. J. Torres, A. Criado, J. C. Palomares and J. Aznar, *J. Clin. Microbiol.*, 38 (2000) 3194

28. S. Morris, G. H. Bai, P. Suffys, L. Portillo-Gomez, M. Fairchok and D. Rouse, *J. Infect. Dis.*, 171 (1995) 954
29. A.S. Lee, I. H. Lim, L. L. Tang, A. Telenti and S. Y. Wong, *Antimicrob. Agents Chemother.*, 43 (1999) 2087
30. P. Kiepiela, K. S. Bishop, A. N. Smith, L. Roux and D. F. York, *Tuber. Lung Dis.*, 80 (2000) 47
31. J. M. Musser, V. Kapur, D. L. Williams, B. N. Kreiswirth, D. vanSoolingen and J. D. A. vanEmbden, *J. Infect. Dis.*, 173 (1996) 196
32. D. A. Rouse, Z. Li, G. H. Bai and S. L. Morris, *Antimicrob. Agents Chemother.*, 39 (1995) 2472
33. A. Milano, E. De Rossi, L. Gusberty, B. Heym, P. Marone and G. Riccardi, *Mol. Microbiol.*, 19 (1996) 113
34. D. A. Rozwarski, G. A. Grant, D. H. Barton, W. R. Jacobs, Jr. and J. C. Sacchettini, *Science*, 279 (1998) 98
35. L. Miesel, T. R. Weisbrod, J. A. Marcinkeviciene, R. Bittman and W. R. Jacobs, Jr., *J. Bacteriol.*, 180 (1998) 2459
36. A. Dessen, A. Quemard, J. S. Blanchard, W. R. Jacobs, Jr. and J. C. Sacchettini, *Science*, 267 (1995) 1638
37. J. S. Oliveira, J. H. Pereira, F. Canduri, N. C. Rodrigues, O. N. de Souza, W. F. de Azevedo, Jr., L. A. Basso and D. S. Santos, *J. Mol. Biol.*, 359 (2006) 646
38. M. V. Dias, I. B. Vasconcelos, A. M. Prado, V. Fadel, L. A. Basso, W. F. de Azevedo, Jr. and D. S. Santos, *J. Struct. Biol.*, 159 (2007) 369
39. S. Sengupta and S. A. Thomas, *Expert Rev. Anticancer Ther.*, 6 (2006) 1433
40. M. Campillos, M. Kuhn, A. C. Gavin, L. J. Jensen and P. Bork, *Science*, 321 (2008) 263
41. M. Malaisree, T. Rungrotmongkol, P. Decha, P. Intharathep, O. Aruksakunwong and S. Hannongbua, *Proteins*, 71 (2008) 1908
42. Y. Yamanishi, M. Araki, A. Gutteridge, W. Honda and M. Kanehisa, *Bioinformatics*, 24 (2008) 1232
43. Z. S. He, J. Zhang, X. H. Shi, L. L. Hu, X. Y. Kong, Y. D. Cai and K. C. Chou, *Plos One*, 5 (2010)
44. M. A. Karimi, A. Hatefi-Mehrjardi, M. Mazloum-Ardakani, R. Behjatmanesh-Ardakani, M. H. Mashhadizadeh and S. Sargazi, *Int. J. Electrochem. Sci.*, 5 (2010) 1634
45. S. Riahi, S. Eynollahi, M. R. Ganjali and P. Norouzi, *Int. J. Electrochem. Sci.*, 5 (2010) 815
46. D. A. Case, T. A. Darden, T. E. Cheatham, 3rd., C. L. Simmerling, J. Wang, J. Wang, R. E. Duke, R. Luo, K. M. Merz, B. Wang, D. A. Pearlman, M. Crowley, S. Brozell, V. Tsui, H. Gohlke, J. Mongan, V. Hornak, G. Cui, P. Beroza, C. Schafmeister, J. W. Caldwell, W. S. Ross and P. A. Kollman, AMBER8, University of California, San Francisco, (2004).
47. Y. Duan, C. Wu, S. Chowdhury, M. C. Lee, G. Xiong, W. Zhang, R. Yang, P. Cieplak, R. Luo, T. Lee, J. Caldwell, J. Wang and P. Kollman, *J Comput Chem*, 24 (2003) 1999
48. T. E. Cheatham, 3rd, P. Cieplak and P. A. Kollman, *J. Biomol. Struct. Dyn.*, 16 (1999) 845
49. W. L. Jorgensen, J. Chandrasekhar, J. D. Madura, R. W. Impey and M. L. Klein, *J. Chem. Phys.*, 79 (1983) 926
50. H. A. Wahab, Y. S. Choong, P. Ibrahim, A. Sadikun and T. Scior, *J. Chem. Inf. Model.*, 49 (2009) 97
51. H. J. C. Berendsen, J. P. M. Postma, W. F. Vangunsteren, A. Dinola and J. R. Haak, *J. Chem. Phys.*, 81 (1984) 3684
52. J. P. Ryckaert, G. Ciccotti and H. J. C. Berendsen, *J. Comput. Phys.*, 23 (1977) 327
53. M. Feig, J. Karanicolas and C. L. Brooks, *J. Mol. Graph. Model.*, 22 (2004) 377
54. J. P. Sun, A. A. Fedorov, S. Y. Lee, X. L. Guo, K. Shen, D. S. Lawrence, S. C. Almo and Z. Y. Zhang, *J Biol Chem*, 278 (2003) 12406
55. M. Pasenkiewicz-Gierula, Y. Takaoka, H. Miyagawa, K. Kitamura and A. Kusumi, *Biophys. J.*, 76 (1999) 1228
56. T. W. Lynch, D. Kosztin, M. A. McLean, K. Schulten and S. G. Sligar, *Biophys. J.*, 82 (2002) 93

57. B. Nguyen, D. Hamelberg, C. Bailly, P. Colson, J. Stanek, R. Brun, S. Neidle and W. D. Wilson, *Biophys. J.*, 86 (2004) 1028
58. S. Pantano, F. Alber, D. Lamba and P. Carloni, *Proteins*, 47 (2002) 62
59. L. A. Basso, R. Zheng, J. M. Musser, W. R. Jacobs, Jr. and J. S. Blanchard, *J. Infect. Dis.*, 178 (1998) 769
60. E. K. Schroeder, L. A. Basso, D. S. Santos and O. N. de Souza, *Biophys. J.*, 89 (2005) 876